Hindawi
Advances in Materials Science and Engineering
Volume 2023, Article ID 9418619, 11 pages
https://doi.org/10.1155/2023/9418619

Research Article

Influence of Recycled Glass on Strength Development of Alkali-Activated High-Calcium Fly Ash Mortar

Nattapong Damrongwiriyanupap,[1] **Sangsan Wongchairattana**,[1] **Tanakorn Phoo-Ngernkham**,[2] **Aruz Petcherdchoo**,[3] **Suchart Limkatanyu**,[4] **and Prinya Chindaprasirt**[5,6]

[1]*Civil Engineering Program, School of Engineering, University of Phayao, Mae Ka, Phayao 56000, Thailand*
[2]*Sustainable Construction Material Technology Research Unit, Department of Civil Engineering, Faculty of Engineering and Technology, Rajamangala University of Technology Isan, Nakhon Ratchasima 30000, Thailand*
[3]*Department of Civil Engineering, Faculty of Engineering, King Mongkut's University of Technology North Bangkok, Bangkok 10800, Thailand*
[4]*Department of Civil Engineering, Faculty of Engineering, Prince of Songkla University, Hat Yai, Songkla 90112, Thailand*
[5]*Sustainable Infrastructure Research and Development Center, Department of Civil Engineering, Faculty of Engineering, Khon Kaen University, Khon Kaen 40002, Thailand*
[6]*Academy of Science, The Royal Society of Thailand, Dusit, Bangkok 10300, Thailand*

Correspondence should be addressed to Tanakorn Phoo-Ngernkham; tanakorn.ph@rmuti.ac.th

Received 21 July 2022; Revised 12 September 2022; Accepted 25 January 2023; Published 20 February 2023

Academic Editor: Andrea Petrella

This article presents the development of green and sustainable mortars using alkali-activated high-calcium fly ash (AAFA) and recycled glass (RG) as part of the fine aggregate. RG was used to replace river sand at dosages of 0%, 25%, 50%, 75%, and 100% by weight. Sodium hydroxide (SH) and sodium silicate (SS) solutions were used as liquid alkaline activators in all mixtures. The AAFA samples were prepared with different liquid-to-binder ratios of 0.6 and 0.7, and the ratio of SS-to-SH was fixed at 2.0. Compressive and flexural strengths were determined at the ages of 7, 28, and 60 days. Test results showed that the compressive and flexural strengths of AAFA mortars declined as RG replacement increased; nevertheless, they increased with curing time. The high Na_2O concentration derived from RG and the weak interfacial transition zone of RG are reasons for the decrease in strength development. The optimum percentage replacement of fine aggregates with RG was found at 25%. The 28-day compressive strength of AAFA with 25% RG was 32.5 MPa for L/B ratios of 0.6 and 29.5 MPa for L/B ratios of 0.7, which resulted in a strength index higher than 75% while releasing low CO_2.

1. Introduction

Recycled glass (RG) is increasingly used for civil engineering applications such as construction backfill material, subbase and subgrade materials, pavement aggregates, trench bedding material, and landfill material. This obviously illustrates the necessity for an alternative approach to glass recycling. The construction industry offers an interesting application of waste glass for concrete, which is an important factor in building and is extensively employed in a variety of countries. Several studies have been conducted to utilize RG as aggregates in concrete [1] as well as using RG powder as partial replacement of cement in concrete [2–5]. Only a few have studied the use of RG as aggregate replacement and as cement partial replacement in ultra-high performance concrete. For example, Yang et al. [6] used RG with a particle size of less than 600 microns as a replacement for 240 microns of silica sand in ultrahigh-performance fibre-reinforced concrete. They reported that the samples with RG had 12% lower compressive strength than the ones with silica sand when

cured at room temperature and 4% lower when cured at 90°C. The average 28-day strength of the samples cured at room temperature was found to be 110 MPa, while those cured at 90°C were 150 MPa. Wille et al. [7] used very fine glass powder (median particle size of 1.7 microns) in the production of ultrahigh-performance concrete with a food-type mixer. They reported that glass powder could be used for cement replacement and that the optimum amount of replacement is 25% of cement by weight. Kou and Xing [8] used 45 microns of RG powder as a cement replacement in ultrahigh-performance concrete. They reported that the replacement of cement with glass powder helped increase the long-term strength of the concrete and that 15% replacement performed better than 30% replacement. Higher strengths were observed for the specimens cured at 90°C in comparison to those cured at 20°C.

However, it is well known that concrete manufacturing is a resource- and energy-intensive process, generating about 5–8% of global greenhouse gas emissions [9–12]. As such, alternatives to decrease its environmental impact are necessary. Nowadays, the use of new binding material i.e. alkali-activated binder (AAB) is one of the ways to reduce CO_2 emissions due to Portland cement production [11, 13, 14]. The AAB can be chemically produced by combining aluminosilicate compounds with alkaline solutions [14–18]. High-calcium fly ash (FA) from the Mae Moh power plant has been utilized as a precursor for AAB production in Thailand due to its extensive availability and acceptable chemical composition [19]. The reaction between SiO_2 and CaO in the FA system assisted in the geopolymerization process when cured at room temperature [20–22]. Hence, a combination of C-S-H (calcium silicate hydrate) and/or C-A-S-H (calcium aluminosilicate hydrate) and N-A-S-H (sodium aluminosilicate hydrate) gels is the main reaction of the high-calcium AAB system [15, 23, 24]. According to Phoo-Ngernkham et al. [25–28], alkali-activated high-calcium FA is a reasonable alternative, especially for repairing works.

As previously mentioned, natural aggregates are limited but extensively used every year. Furthermore, the crushed aggregate for use in the building sector is expensive. Alternatively, it can be seen that using RG as an aggregate in structural concrete has the potential to not only improve the environment due to reducing waste and raw material utilization but also benefit the industry due to lowering costs. The outcome of this research could help not only Thailand but also the world to divert a significant quantity of waste material, i.e., waste glass, from landfills and considerably reduce environmental damage caused by carbon emissions due to PC production. Therefore, in this work, the effect of the incorporation of RG as fine aggregate replacement on the strength development of alkali-activated, high-calcium FA mortar was investigated.

2. Materials and Testing Analysis

High-calcium fly ash (FA) derived from the Mae Moh lignite power plant in northern Thailand was used as a raw material for producing alkali-activated high-calcium FA (AAFA). The FA had a specific gravity of 2.65, a median particle size of 15.5 μm, and Blaine fineness of 3840 cm^2/g. The chemical compositions of FA consisted of SiO2 (25.6%), Al2O3 (9.1%), Fe2O3 (27.8%), CaO (25.0%), MgO (3.0%), K2O (3.0%), Na2O (0.2%), SO3 (3.85%), and LOI (2.54%), as shown in Table 1. The sum of SiO2, Al2O3, and Fe2O3 was 62.5%, and the CaO content was high at 25.0%. This FA was Class C fly ash as specified by ASTM C618 [29]. The XRD patterns of FA and RG are illustrated in Figure 1, whereas their SEM images are shown in Figure 2(a) for FA and Figure 2(b) for RG. 10 molar sodium hydroxide (SH) and sodium silicate (SS) with 13.89% Na2O, 32.15% SiO2, and 53.96% H2O were used as alkali activators. The fine aggregates used in this study were local river sand (RS) and crushed recycled glass (RG). The RS had a specific gravity and fineness modulus of 2.62 and 1.41, respectively, whereas the RG had a specific gravity and fineness modulus of 2.51 and 1.67, respectively.

The abbreviations FA-0RG, FA-25RG, FA-50RG, FA-75RG, and FA-100RG indicate AAFA mortars containing the RS replacement with RG at 0%, 25%, 50%, 75%, and 100% by weight, respectively. The ratios of liquid to solid binder (L/B) were varied between 0.6 and 0.7. While the ratios of SS-to-SH and sand-to-binder were fixed at 2.0.

In the mixing process of AAFA mortars, FA and RS/RG were dry-mixed until the mixture was homogeneous, which took approximately 1 minute. The alkali activator solutions were then added and mixed for an additional 3 minutes. After mixing, fresh mortars were then placed into $50 \times 50 \times 50$ mm cube and $75 \times 75 \times 300$ mm prism molds for compressive [30] and flexural [31] strength tests, respectively. To prevent moisture loss, the specimens were covered with a vinyl sheet and stored in a 25°C controlled room for 7, 28, and 60 days prior to the day of testing. In the results, three samples were tested and averaged. Table 2 lists the mix proportions and setting time results of AAFA mortar under different RG contents. According to Table 2, it is found that the setting time of AAFA tended to increase marginally as RG content increased. In addition, an increase in their L/B ratios could prolong their setting times. This is agreed with the works of Sinsiri et al. [20].

3. Results and Discussion

3.1. Compressive Strength. The compressive strength of AAFA mortars under different L/B ratios at various amount of RS replacement with RG is summarized in Figure 3. As seen in Figure 3, the compressive strength of mortar specimens depends on the L/B ratio and percentage of RG content in the mixtures. At 7 days, it is evident that compressive strength of specimens slightly decreased with increasing the amount of RG replacement for both L/B ratios of 0.6 and 0.7. For example, the compressive strengths of FA-0RG, FA-25RG, FA-50RG, FA-75RG, and FA-100RG mortars at the L/B ratio of 0.60 are 16.9, 16.6, 16.4, and 14.5 MPa, respectively. The highest compressive strength of mortar was obtained at the reference mortar (0% RG replacement), which was 17.8 and 13.2 MPa for L/B ratios of 0.6 and 0.7, respectively. The significant decrease in strength

Table 1: Chemical compositions of FA, RS, and RG (by % weight).

Materials	SiO_2	Al_2O_3	Fe_2O_3	CaO	MgO	K_2O	Na_2O	Other	SO_3	LOI
FA	25.56	9.05	27.79	24.97	0.46	3.01	0.16	2.61	3.85	2.54
RS	92.00	1.60	0.60	0.90	0.10	2.20	0.10	—	—	2.10
RG	65.80	1.33	0.17	12.00	1.29	0.17	12.90	5.76	0.13	0.45

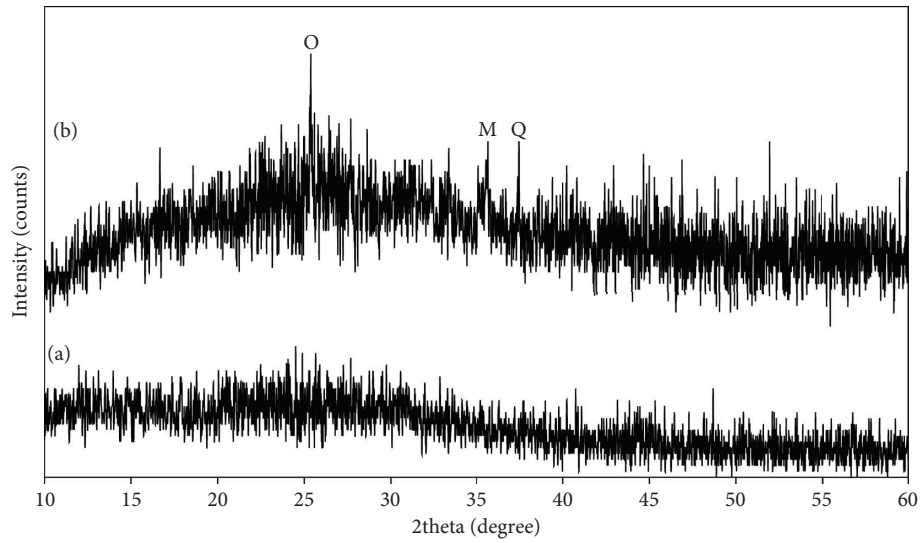

Figure 1: XRD patterns of materials: (a) RG and (b) FA (o = calcium sulfate ($CaSO_4$), M = magnesioferrite ($MgFe_2O_4$), and Q = quartz (SiO_2)).

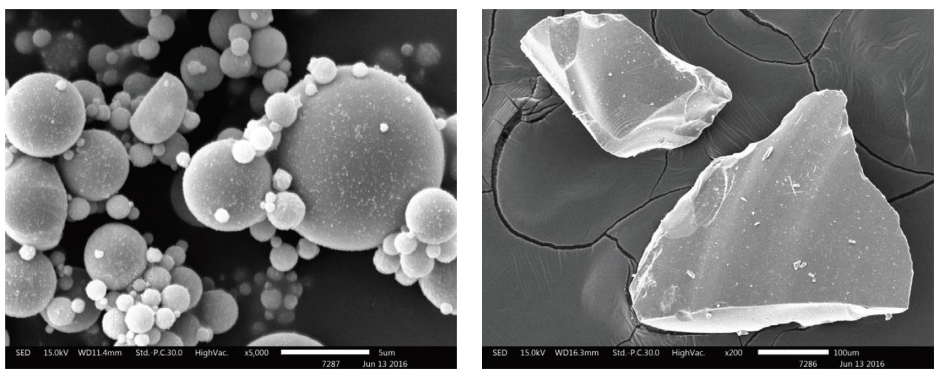

(a) (b)

Figure 2: SEM images of (a) FA and (b) RG.

development occurred due to a weaker interfacial transition zone in the mortar with RG. Ling and Poon [32] also reported that the reduction in bonding between aggregates and paste occurred due to the smoother surface of RG compared to that of RS. Also, the effect of the Na_2O concentration (see Table 1) played a significant role in the development of its strength. Detphan et al. [33] claimed that the excess Na_2O content in the matrix induced a slow reaction rate during the geopolymerization process. Zhang et al. [34] demonstrated that higher Na_2O content resulted in higher drying shrinkage of alkali-activated binder, which might result in microcracks and thus strength loss. Note that the use of RG in AAM might induce the alkali-silica reaction (ASR) within the matrix [34]. However, the ASR expansion could be controlled by incorporating additional aluminium sources and adjusting the RG to binder ratio in the mixtures. Consideration should be given to this ASR for the usage of AAFA with RG in construction works.

At 28 days, the samples with 25% RG replacement provided the highest strengths of 32.5 and 29.5 MPa for L/B ratios of 0.6 and 0.7, respectively. However, when the amount of RG replacement exceeded 25%, the compressive strength of AAFA mortars obviously decreased. This is agreed with the SEM images of a 28-day-cured AAFA, as shown in Figure 4. According to Figure 4, increasing the RG replacement content had a detrimental effect on the strength

Table 2: Mix proportions of alkali-activated high-calcium FA mortars with RG (kg/m^3).

Mix no.	Mix symbol	L/B ratio	FA (kg)	RS (kg)	RG (kg)	NH (kg)	NS (kg)	Setting time (min)	
								Initial	Final
1	FA-0RG	0.60	862.0	862.0	—	172.4	344.8	20	37
2	FA-25RG		859.0	644.3	343.6	171.8	343.6	20	38
3	FA-50RG		856.0	428.0	428.0	171.2	342.4	22	38
4	FA-75RG		853.0	213.3	639.8	170.6	341.2	23	40
5	FA-100RG		850.0	—	850.0	170.0	340.0	24	42
6	FA-0RG	0.70	815.0	815.0	—	190.2	380.3	27	48
7	FA-25RG		813.0	609.8	203.3	189.7	379.4	28	50
8	FA-50RG		810.0	405.0	405.0	189.0	378.0	30	50
9	FA-75RG		807.0	201.8	605.3	188.3	376.6	32	52
10	FA-100RG		804.0	—	804.0	187.6	375.2	33	52

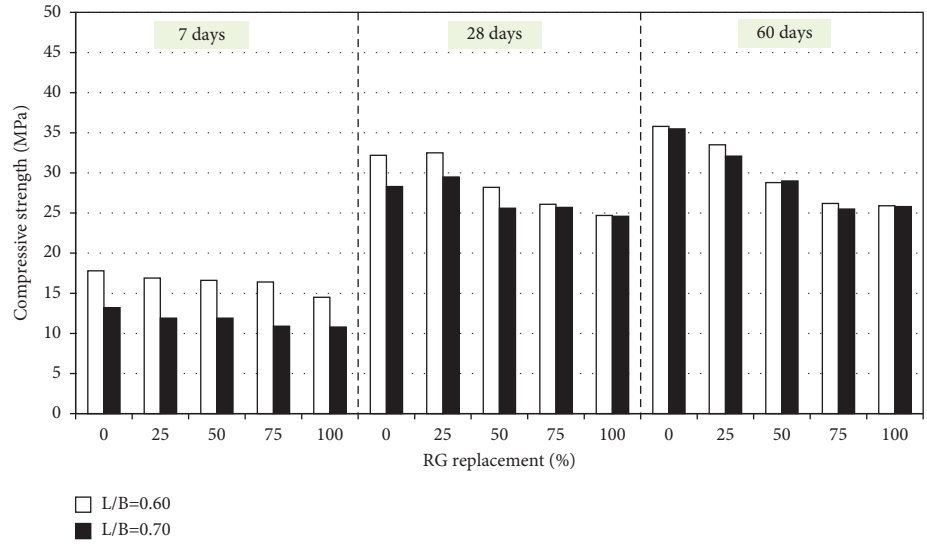

Figure 3: Compressive strength of AAFA mortar containing RG under different curing times and L/B ratios.

development of the composites owing to the formation of poor pore structures. Note that the 28-day and 60-day compressive strengths of specimens were higher than the 7-day compressive strength due to the increase in geopolymerization degree, as confirmed by several publications [20, 26, 35–37]. Additionally, the reaction between SiO2 and/or Al2O3 and CaO in the high-calcium FA system facilitated the formation of calcium aluminosilicate hydrate (C-A-S-H) in the matrix [20, 38, 39], resulting in later strength development.

Figure 5 shows the relationship between normalized compressive strength and curing time of AAFA mortar containing RG at the 28-day compressive strength. As seen in Figure 5, the strength development of mortars with RG increased gradually as the curing period increased. The correlation between normalized compressive strength and curing time of RG mortars was shown using the 28-day compressive strength as the logarithm function. This empirical equation has been effectively used to materials based on cement materials and alkali-activated binder [16, 40, 41]. The compressive strengths of AAFA mortars can be described empirically in terms of curing durations, as seen in equation (1) and displayed in Figure 5. The constants in equation (1) were derived by curve-fitting the findings of RG contents at 0%, 25%, 50%, 75%, and 100%. The curve fitting produced an R^2 value of 0.892, which is good for engineering applications

$$\frac{f'_{c,d}}{f'_{c,28}} = 0.27453 \ln(d) + 0.00258, \quad (1)$$

where $f'_{c,d}$ is the compressive strength at d days of curing time and $f'_{c,28}$ is the compressive strength at 28 days of curing time.

3.2. Flexural Strength. The flexural strength of AAFA mortars at different L/B ratios cured for 7, 28, and 60 days is illustrated in Figure 6. The flexural strength of mortars exhibited a similar trend to the compressive strength results. The trend of flexural strength seemed to decline with increasing RS replacement with RG. For example, at an L/B ratio of 0.60 and a curing time of 28 days, the flexural strengths of FA-25RG, FA-50RG, FA-75RG, and FA-100RG mortars were 0.51, 0.22, 0.12, and 0.10 MPa, respectively. While the highest 28-day flexural strength of FA-0RG

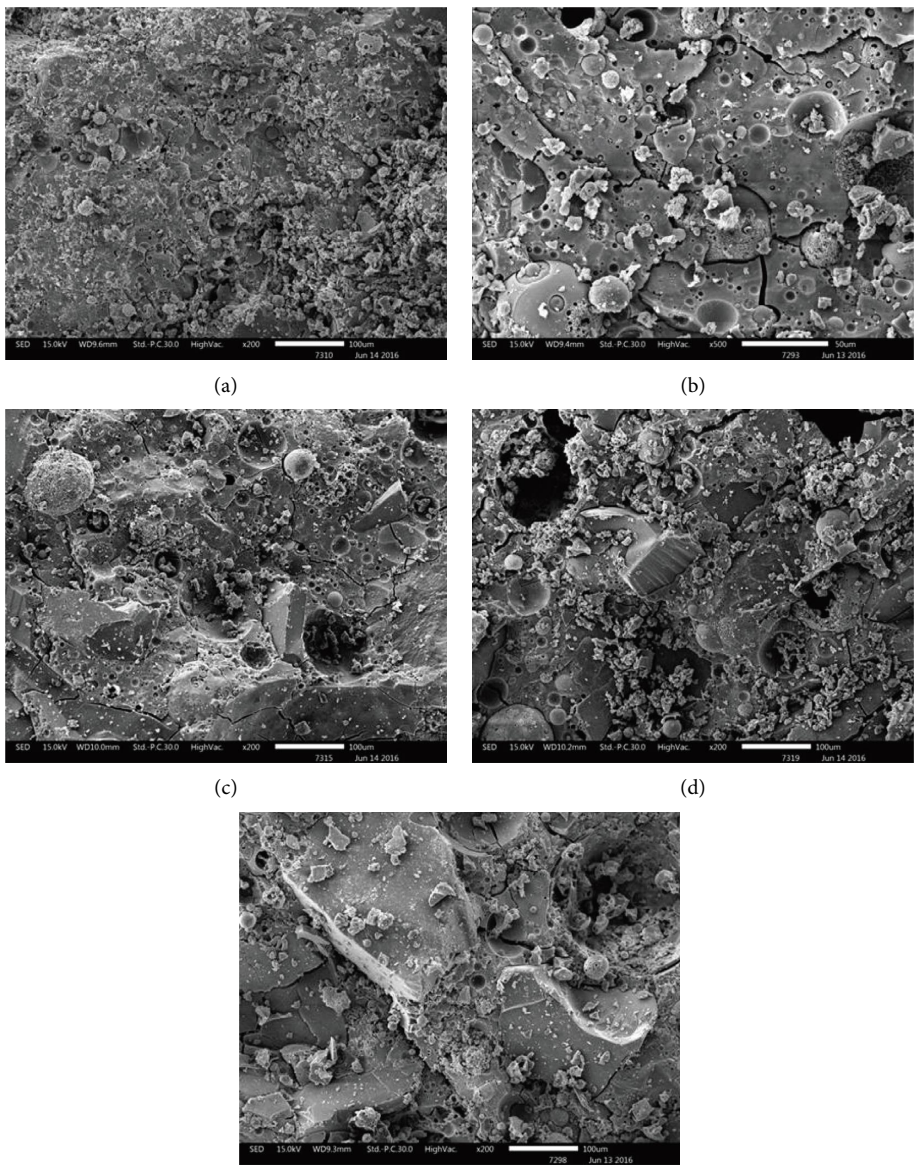

Figure 4: SEM images of a 28-day-cured AAFA: (a) FA-0RG, (b) FA-25RG, (c) FA-50RG, (d) FA-75RG, and (e) FA-100RG.

mortar was 1.05 MPa for L/B ratios of 0.60. As seen in Figure 6, the flexural strength of mortars with 25% RG replacement was slightly reduced. And also, they declined significantly as RG replacement increased. The decline in flexural strength may be related to the replacement of RG, which increases the Na2O content in the matrix due to its high Na2O composition (see Table 1). As explained previously, a greater Na2O molar ratio increased its drying shrinkage [34], resulting in the formation of many microcracks. In addition, increasing of Na2O content induced the alkali-silica reaction (ASR) in the alkali-activated binder system, as reported by Long et al. [42] and Idir et al. [43]. Previous publications [42, 44, 45] reported that the ASR growth was first inhibited owing to the consumption of OH-ions in the pore solution. And, when the SiO2 was gradually consumed, the Na2O in the pore solution reacted with the RG. This probably led to the occurrence of the ASR. This observation can be confirmed by using the XRD patterns of a 28-day-cured AAFA, as illustrated in Figure 7. It is found that all AAFA mortars mainly consist of crystalline phases of quartz (SiO_2). Moreover, Tho-In et al. [46] demonstrated that the friction between RG and the paste within the matrix had a negative effect on its strength development.

Figure 8 shows the relationship between normalized flexural strength and curing time of AAFA mortar containing RG based on consideing the 28-day flexural strength equation (2) illustrates an empirical relationship between the flexural strength of mortars containing RG and the curing time at various L/B ratios, with a high R^2 value of 0.752. The constants in equation (2) were determined by curve-fitting the data for RG replacement levels of 0%, 25%, 50%, 75%, and 100%:

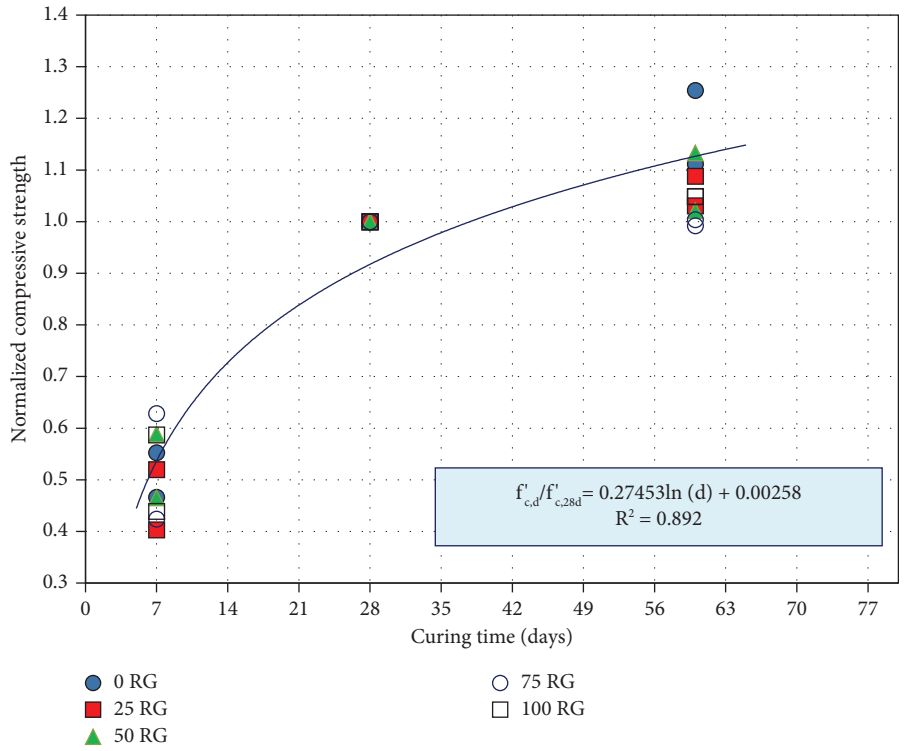

Figure 5: Relationship between normalized compressive strength and curing time of AAFA mortar containing RG by the 28-day compressive strength.

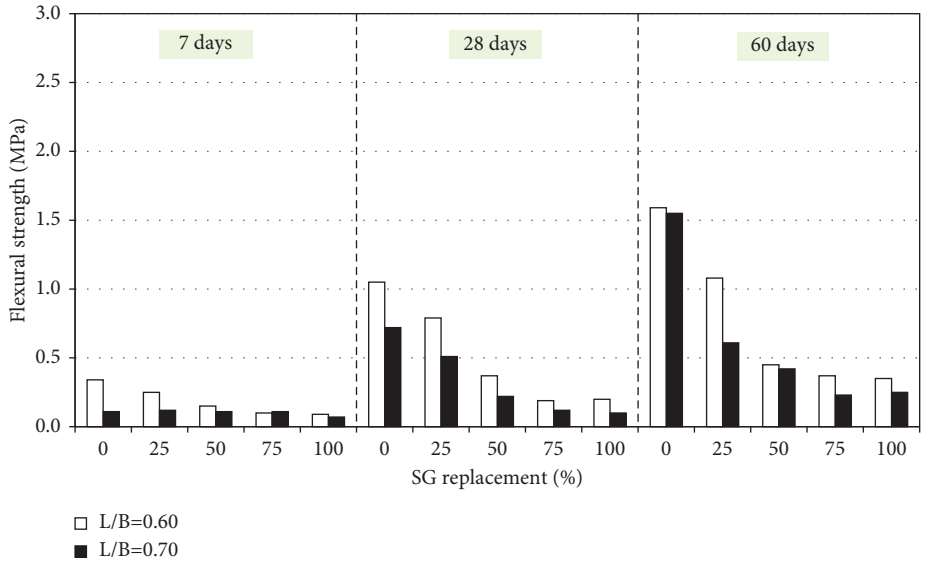

Figure 6: Flexural strength of AAFA mortar containing RG under different curing times and L/B ratios.

$$\frac{f_{t,d}}{f_{t,28}} = 0.57720 \ln (d) - 0.73670, \quad (2)$$

where $f_{t,d}$ is the flexural strength at d days of curing time and $f_{t,28}$ is the flexural strength at 28 days of curing time.

3.3. Life-Cycle Assessment. The life-cycle assessment (LCA) of AAFA mortars incorporating SG was evaluated. According to previous publications [27, 47], the measurement unit of emission in the LCA analysis is CO_2-e emitted (t CO_2-e/m^3). Table 3 shows the emission factors obtained from the

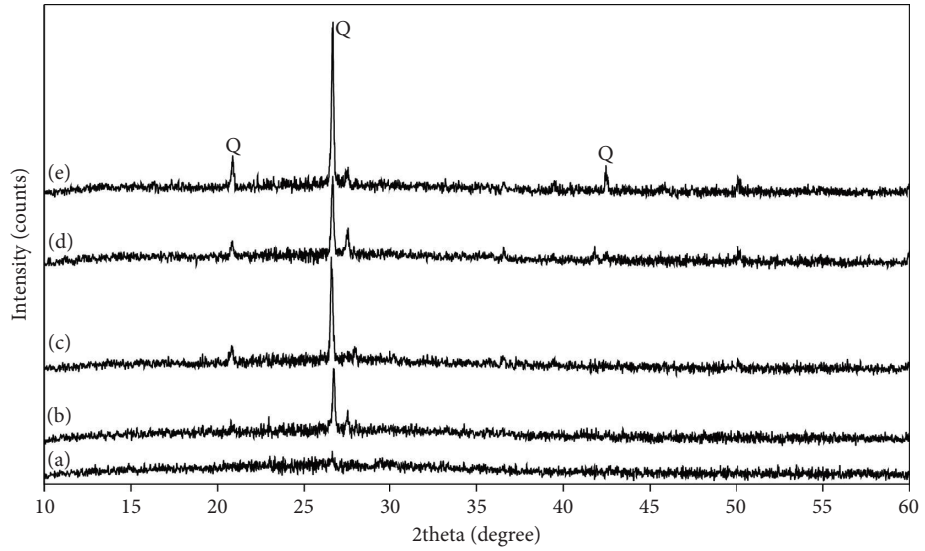

Figure 7: XRD patterns of a 28-day-cured AAFA: (a) FA-100RG, (b) FA-75RG, (c) FA-50RG, (d) FA-25RG, and (e) FA-0RG (Q = quartz (SiO_2)).

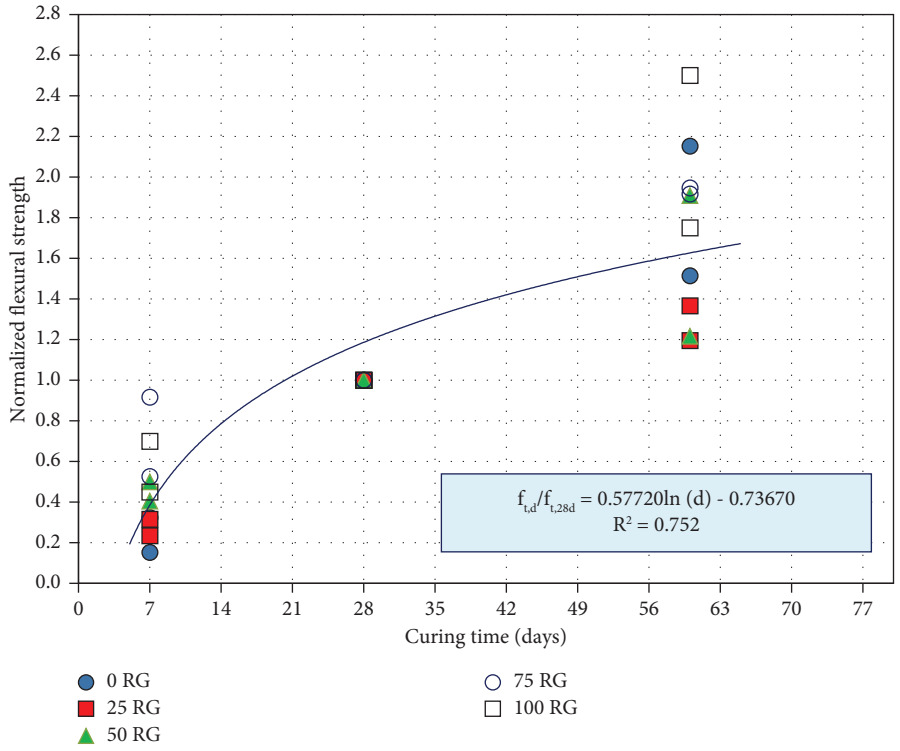

Figure 8: Relationship between normalized flexural strength and curing time of AAFA mortar containing RG by the 28-day flexural strength.

Table 3: The emission factors of tested materials [13, 48–50].

Materials (kg)	Emission factor (t CO_2-e/m^3)
Portland cement, PC	0.8200
High-calcium fly ash, FA	0.0070
River sand, RS	0.0139
Recycled glass, RG	0.0200
Coase aggregate, CA	0.4300
Sodium hydroxide, SH	0.7000
Sodium silicate, SS	1.5140

literature [13, 48–50]. However, the emission factors derived from various studies, especially those conducted in different regions or countries, may vary significantly. The further use of results should be done with care. According to Table 3, FA emitted the least CO_2, while SS solution emitted the highest values. The LCA analyses for AAFA mortars incorporating SG and Portland cement mortar (PCM) are shown in Tables 4 and 5. It is revealed when the RG replacement level increased, the CO_2-e emitted values tended to marginal increase. According to Tables 4 and 5, AAFA mortars emitted lower

Table 4: LCA analysis of AAFA mortar incorporating RG from this article.

L/B ratios	Mix symbol	FA (kg)	CO_2-e/m^3 from FA	RS (kg)	CO_2-e/m^3 from RS	RG (kg)	CO_2-e/m^3 from RG	SH (kg)	CO_2-e/m^3 from SH	SS (kg)	CO_2-e/m^3 from SS	Total CO_2-e/m^3
0.60	FA-0RG	862.0	0.0060	862.0	0.0120	—	0.0000	172.4	0.0362	344.8	0.2245	0.27869
	FA-25RG	859.0	0.0060	644.3	0.0090	343.6	0.0069	171.8	0.0361	343.6	0.2237	0.28161
	FA-50RG	856.0	0.0060	428.0	0.0059	428.0	0.0086	171.2	0.0360	342.4	0.2229	0.27936
	FA-75RG	853.0	0.0060	213.3	0.0030	639.8	0.0128	170.6	0.0358	341.2	0.2221	0.27969
	FA-100RG	850.0	0.0060	—	—	850.0	0.0170	170.0	0.0357	340.0	0.2213	0.28000
0.70	FA-0RG	815.0	0.0057	815.0	0.0113	—	0.0000	190.2	0.0399	380.3	0.2476	0.30456
	FA-25RG	813.0	0.0057	609.8	0.0085	203.3	0.0041	189.7	0.0398	379.4	0.2470	0.30507
	FA-50RG	810.0	0.0057	405.0	0.0056	405.0	0.0081	189.0	0.0397	378.0	0.2461	0.30518
	FA-75RG	807.0	0.0056	201.8	0.0028	605.3	0.0121	188.3	0.0395	376.6	0.2452	0.30528
	FA-100RG	804.0	0.0056	—	—	804.0	0.0161	187.6	0.0394	375.2	0.2443	0.30537

Table 5: LCA analysis of PCC and PCM.

Mix symbol	PC (kg)	CO_2-e/m^3 from PC	RS (kg)	CO_2-e/m^3 from RS	CA (kg)	CO_2-e/m^3 from CA	Total CO_2-e/m^3
PCC	495.0	0.4059	510.0	0.0071	938.0	0.4033	0.8163
PCM (w/c = 0.60)	596.0	0.4887	1192.0	0.0166	—	—	0.5053
PCM (w/c = 0.70)	562.0	0.4608	1123.0	0.0156	—	—	0.4765

CO_2 than PCMs. For example, the CO_2-e emitted values of FA-25RG and PCM were 0.28161 and 0.5053 ton CO_2-e/ton, respectively, for L/B ratios of 0.60 and w/c ratios of 0.60. In addition, all AAFA mortars generated lower CO_2 than Portland cement concrete (PCC). Note that the 28-day compressive strengths of PCMs were 46.2 and 37.1 MPa for w/c ratios of 0.60 and 0.70, respectively. While the 28-day compressive strength of PCC was 35.5 MPa. As shown in Figure 3, the strengths of AAFA mortars were slightly lower than those of PCM and PCC. As shown in Tables 4 and 5, the FA content of the AAFA mortar is around 800 kg/m^3, while the PC content of the PCM mortar is approximately 600 kg/m^3. However, PC is approximately 2 times more expensive than FA, according to Thailand market prices (2022) and Phoo-Ngernkham et al. [27]. Therefore, the relatively large amount of FA used in the production of AAFA has no significant effect on the total price of AAFA. According to the basis of empirical evidence, it is recommended that 25% RG be used in replacement of RS as fine aggregate in order to have a strength index greater than 75% and a low carbon footprint. For further studies, it is recommended to apply the findings in this study to construction practice [51, 52] and also compare them to other materials [53, 54].

4. Conclusion

This article investigated the compressive and flexural strengths of FA-based alkali-activated mortar mixed with RG. Here, RG was used to partially replace fine aggregate in the amounts of 0%, 25%, 50%, 75%, and 100% by weight. The results showed that the compressive and flexural strengths decreased with the increased amount of RG replacement. The reduction in strength development occurred because of the weaker interfacial transition zone of RG in mortars. Additionally, high Na_2O content resulted in greater drying shrinkage of the alkali-activated binder, which might result in microcracks and subsequent strength loss. The increasing Na2O concentration could induce the alkali-silica reaction (ASR) in the alkali-activated binder system because all AAFA mortars consist mostly of quartz crystalline phases (SiO2). The use of 25% RG in AAFA mortar at a L/B ratio of 0.60 is a feasible choice for sustainable concrete because the 28-day compressive and flexural strengths of AAFA incorporating 25% RG were 32.5 and 1.08 MPa for L/B ratios of 0.60, while those of AAFA without RG were 35.8 and 1.59 MPa. Hence, it provides a strength index greater than 75% while emitting little CO_2.

Data Availability

The data used to support the findings of this study are available from the corresponding author upon request.

Conflicts of Interest

The authors declare that they have no conflicts of interest.

Acknowledgments

This work was financially supported by the (TRF) New Research Scholar (Grant no. MRG6180056) and the TRF Senior Research Scholar (Grant no. RTA6280012). This research was also funded by the National Science, Research and Innovation Fund (NSRF), and King Mongkut's University of Technology North Bangkok with contract no. KMUTNB-FF-66-09. The last author would like to acknowledge the "Support by Research and Graduate Studies" Khon Kaen University.

References

[1] S. B. Park, B. C. Lee, and J. H. Kim, "Studies on mechanical properties of concrete containing waste glass aggregate," *Cement and Concrete Research*, vol. 34, no. 12, pp. 2181–2189, 2004.

[2] A. Shayan and A. Xu, "Value-added utilisation of waste glass in concrete," *Cement and Concrete Research*, vol. 34, no. 1, pp. 81–89, 2004.

[3] C. Shi, Y. Wu, C. Riefler, and H. Wang, "Characteristics and pozzolanic reactivity of glass powders," *Cement and Concrete Research*, vol. 35, no. 5, pp. 987–993, 2005.

[4] A. Shayan and A. Xu, "Performance of glass powder as a pozzolanic material in concrete: a field trial on concrete slabs," *Cement and Concrete Research*, vol. 36, no. 3, pp. 457–468, 2006.

[5] N. Schwarz, H. Cam, and N. Neithalath, "Influence of a fine glass powder on the durability characteristics of concrete and its comparison to fly ash," *Cement and Concrete Composites*, vol. 30, no. 6, pp. 486–496, 2008.

[6] S. L. Yang, S. G. Millard, M. N. Soutsos, S. J. Barnett, and T. T. Le, "Influence of aggregate and curing regime on the mechanical properties of ultra-high performance fibre reinforced concrete (UHPFRC)," *Construction and Building Materials*, vol. 23, no. 6, pp. 2291–2298, 2009.

[7] K. Wille, A. E. Naaman, and G. J. Parra-Montesinos, "Ultra-high performance concrete with compressive strength exceeding 150 MPa (22 ksi): a simpler way," *ACI Materials Journal*, vol. 108, no. 1, 2011.

[8] S. C. Kou and F. Xing, "The effect of recycled glass powder and reject fly ash on the mechanical properties of fibre-reinforced ultrahigh performance concrete," *Advances in Materials Science and Engineering*, vol. 2012, Article ID 263243, 8 pages, 2012.

[9] K. L. Scrivener and R. J. Kirkpatrick, "Innovation in use and research on cementitious material," *Cement and Concrete Research*, vol. 38, no. 2, pp. 128–136, 2008.

[10] G. Habert, J. B. d'Espinose de Lacaillerie, and N. Roussel, "An environmental evaluation of geopolymer based concrete

production: reviewing current research trends," *Journal of Cleaner Production*, vol. 19, no. 11, pp. 1229–1238, 2011.

[11] B. C. McLellan, R. P. Williams, J. Lay, A. Van Riessen, and G. D. Corder, "Costs and carbon emissions for geopolymer pastes in comparison to ordinary portland cement," *Journal of Cleaner Production*, vol. 19, no. 9–10, pp. 1080–1090, 2011.

[12] J. Suebsuk, S. Horpibulsuk, A. Suksan, C. Suksiripattanapong, T. Phoo-ngernkham, and A. Arulrajah, "Strength prediction of cement-stabilised reclaimed asphalt pavement and lateritic soil blends," *International Journal of Pavement Engineering*, vol. 20, no. 3, pp. 332–338, 2019.

[13] N. Damrongwiriyanupap, T. Srikhamma, C. Plongkrathok et al., "Assessment of equivalent substrate stiffness and mechanical properties of sustainable alkali-activated concrete containing recycled concrete aggregate," *Case Studies in Construction Materials*, vol. 16, Article ID e00982, 2022.

[14] C. Detphan, P. Kaeorawang, B. Injorhor et al., "Improving drying shrinkage and strength development of alkali-activated high-calcium fly ash using commercial-grade calcium sulfate as expansive additive," *Engineering and Applied Science Research*, vol. 49, no. 1, pp. 58–64, 2022.

[15] F. Pacheco-Torgal, J. Castro-Gomes, and S. Jalali, "Alkali-activated binders: a review," *Construction and Building Materials*, vol. 22, no. 7, pp. 1305–1314, 2008.

[16] N. Damrongwiriyanupap, A. Wachum, K. Khansamrit et al., "Improvement of recycled concrete aggregate using alkali-activated binder treatment," *Materials and Structures*, vol. 55, no. 1, p. 11, 2021.

[17] T. Xie, P. Visintin, X. Zhao, and R. Gravina, "Mix design and mechanical properties of geopolymer and alkali activated concrete: review of the state-of-the-art and the development of a new unified approach," *Construction and Building Materials*, vol. 256, Article ID 119380, 2020.

[18] T. Xie and T. Ozbakkaloglu, "Influence of coal ash properties on compressive behaviour of FA- and BA-based GPC," *Magazine of Concrete Research*, vol. 67, no. 24, pp. 1301–1314, 2015.

[19] D. Intarabut, P. Sukontasukkul, T. Phoo-ngernkham et al., "Influence of graphene oxide nanoparticles on bond-slip reponses between fiber and geopolymer mortar," *Nanomaterials*, vol. 12, no. 6, p. 943, 2022.

[20] T. Sinsiri, T. Phoo-ngernkham, V. Sata, and P. Chindaprasirt, "The effects of replacement fly ash with diatomite in geopolymer mortar," *Computers and Concrete*, vol. 9, no. 6, pp. 427–437, 2012.

[21] A. Wongkvanklom, P. Posi, P. Kasemsiri, V. Sata, T. Cao, and P. Chindaprasirt, "Strength, thermal conductivity and sound absorption of cellular lightweight high calcium fly ash geopolymer concrete," *Engineering and Applied Science Research*, vol. 48, no. 4, pp. 487–496, 2021.

[22] A. Wongkvanklom, V. Sata, J. G. Sanjayan, and P. Chindaprasirt, "Setting time, compressive strength and sulfuric acid resistance of a high calcium fly ash geopolymer containing borax," *Engineering and Applied Science Research*, vol. 45, no. 2, pp. 89–94, 2018.

[23] I. Garcia-Lodeiro, A. Fernandez-Jimenez, and A. Palomo, "Hydration kinetics in hybrid binders: early reaction stages," *Cement and Concrete Composites*, vol. 39, no. 0, pp. 82–92, 2013.

[24] P. Chindaprasirt, T. Phoo-ngernkham, S. Hanjitsuwan, S. Horpibulsuk, A. Poowancum, and B. Injorhor, "Effect of calcium-rich compounds on setting time and strength development of alkali-activated fly ash cured at ambient temperature," *Case Studies in Construction Materials*, vol. 9, Article ID e00198, 2018.

[25] T. Phoo-Ngernkham, P. Chindaprasirt, V. Sata, S. Hanjitsuwan, and S. Hatanaka, "The effect of adding nano-SiO_2 and nano-Al_2O_3 on properties of high calcium fly ash geopolymer cured at ambient temperature," *Materials and Design*, vol. 55, no. 0, pp. 58–65, 2014.

[26] T. Phoo-ngernkham, S. Hanjitsuwan, L. Y. Li, N. Damrongwiriyanupap, and P. Chindaprasirt, "Adhesion characterisation of Portland cement concrete and alkali-activated binders," *Advances in Cement Research*, vol. 31, no. 2, pp. 69–79, 2019.

[27] T. Phoo-Ngernkham, C. Phiangphimai, D. Intarabut et al., "Low cost and sustainable repair material made from alkali-activated high-calcium fly ash with calcium carbide residue," *Construction and Building Materials*, vol. 247, Article ID 118543, 2020.

[28] T. Phoo-ngernkham, V. Sata, S. Hanjitsuwan, C. Ridtirud, S. Hatanaka, and P. Chindaprasirt, "High calcium fly ash geopolymer mortar containing Portland cement for use as repair material," *Construction and Building Materials*, vol. 98, pp. 482–488, 2015.

[29] Astm C618-15, "Standard specification for coal fly ash and raw or calcined natural pozzolan for use in concrete," *Annual Book of ASTM Standards*, vol. 04.02, 2015.

[30] Astm C109, "Standard test method of compressive strength of hydrualic cement mortars (using 2-in. or [50 mm] cube speciments)," *Annual Book of ASTM Standard*, vol. 04.01, 2002.

[31] Astm C293-02, "Flexural strength of concrete (using simple beam with center-point loading)," *Annual Book of ASTM Standard*, vol. 04.02, 2002.

[32] T. C. Ling and C. S. Poon, "Properties of architectural mortar prepared with recycled glass with different particle sizes," *Materials and Design*, vol. 32, no. 5, pp. 2675–2684, 2011.

[33] S. Detphan, C. Phiangphimai, A. Wachum, S. Hanjitsuwan, T. Phoo-ngernkham, and P. Chindaprasirt, "Strength development and thermal conductivity of POFA lightweight geopolymer concrete incorporating FA and PC," *Engineering and Applied Science Research*, vol. 48, no. 6, pp. 718–723, 2021.

[34] B. Zhang, P. He, and C. S. Poon, "Optimizing the use of recycled glass materials in alkali activated cement (AAC) based mortars," *Journal of Cleaner Production*, vol. 255, Article ID 120228, 2020.

[35] T. Phoo-ngernkham, P. Chindaprasirt, V. Sata, and T. Sinsiri, "High calcium fly ash geopolymer containing diatomite as additive," *Indian Journal of Engineering and Materials Sciences*, vol. 20, no. 4, pp. 310–318, 2013.

[36] C. Suksiripattanapong, S. Horpibulsuk, C. Phetchuay, J. Suebsuk, T. Phoo-ngernkham, and A. Arulrajah, "Water treatment sludge-calcium carbide residue geopolymers as nonbearing masonry units," *Journal of Materials in Civil Engineering*, vol. 29, no. 9, 2017.

[37] P. Sukontasukkul, P. Chindaprasirt, P. Pongsopha, T. Phoo-Ngernkham, W. Tangchirapat, and N. Banthia, "Effect of fly ash/silica fume ratio and curing condition on mechanical properties of fiber-reinforced geopolymer," *Journal of Sustainable Cement-Based Materials*, vol. 9, no. 4, pp. 218–232, 2020.

[38] I. Garcia-Lodeiro, A. Palomo, A. Fernandez-Jimenez, and D. E. MacPhee, "Compatibility studies between N-A-S-H and C-A-S-H gels. Study in the ternary diagram Na2O-CaO-Al2O3-SiO 2-H2O," *Cement and Concrete Research*, vol. 41, no. 9, pp. 923–931, 2011.

[39] X. Guo, H. Shi, and W. A. Dick, "Compressive strength and microstructural characteristics of class C fly ash geopolymer," *Cement and Concrete Composites*, vol. 32, no. 2, pp. 142–147, 2010.

[40] K. Chaidachatorn, J. Suebsuk, S. Horpibulsuk, and A. Arulrajah, "Extended water/cement ratio law for cement mortar containing recycled asphalt pavement," *Construction and Building Materials*, vol. 196, pp. 457–467, 2019.

[41] G. Rao, "Generalization of Abrams' law for cement mortars," *Cement and Concrete Research*, vol. 31, no. 3, pp. 495–502, 2001.

[42] W. J. Long, X. Zhang, J. Xie et al., "Recycling of waste cathode ray tube glass through fly ash-slag geopolymer mortar," *Construction and Building Materials*, vol. 322, Article ID 126454, 2022.

[43] R. Idir, M. Cyr, and A. Pavoine, "Investigations on the durability of alkali-activated recycled glass," *Construction and Building Materials*, vol. 236, Article ID 117477, 2020.

[44] W. Aiqin, Z. Chengzhi, T. Mingshu, and Z. Ningsheng, "ASR in mortar bars containing silica glass in combination with high alkali and high fly ash contents," *Cement and Concrete Composites*, vol. 21, no. 5-6, pp. 375–381, 1999.

[45] A. Gholizadeh Vayghan, F. Rajabipour, and J. L. Rosenberger, "Composition–rheology relationships in alkali–silica reaction gels and the impact on the gel's deleterious behavior," *Cement and Concrete Research*, vol. 83, pp. 45–56, 2016.

[46] T. Tho-In, V. Sata, K. Boonserm, and P. Chindaprasirt, "Compressive strength and microstructure analysis of geopolymer paste using waste glass powder and fly ash," *Journal of Cleaner Production*, vol. 172, pp. 2892–2898, 2018.

[47] T. Phoo-ngernkham, S. Hanjitsuwan, C. Suksiripattanapong, J. Thumrongvut, J. Suebsuk, and S. Sookasem, "Flexural strength of notched concrete beam filled with alkali-activated binders under different types of alkali solutions," *Construction and Building Materials*, vol. 127, pp. 673–678, 2016.

[48] D. A. Turner, I. D. Williams, and S. Kemp, "Greenhouse gas emission factors for recycling of source-segregated waste materials," *Resources, Conservation and Recycling*, vol. 105, pp. 186–197, 2015.

[49] L. K. Turner and F. G. Collins, "Carbon dioxide equivalent (CO_2-e) emissions: a comparison between geopolymer and OPC cement concrete," *Construction and Building Materials*, vol. 43, no. 0, pp. 125–130, 2013.

[50] F. G. Collins, "Inclusion of carbonation during the life cycle of built and recycled concrete: influence on their carbon footprint," *International Journal of Life Cycle Assessment*, vol. 15, no. 6, pp. 549–556, 2010.

[51] A. Petcherdchoo, "Probability-based sensitivity of service life of chloride-attacked concrete structures with multiple cover concrete repairs," *Advances in Civil Engineering*, vol. 2018, Article ID 4525646, 17 pages, 2018.

[52] A. Petcherdchoo, T. Hongubon, N. Thanasisathit, K. Punthutaecha, and S.-H. Jang, "Effect of curing time on bond strength between reinforcement and fly-ash geopolymer concrete," *Applied Science and Engineering Progress*, vol. 13, no. 2, pp. 127–135, 2020.

[53] A. Petcherdchoo, "Service life and environmental impact due to repairs by metakaolin concrete after chloride attack," *RILEM Bookseries*, vol. 10, pp. 35–41, 2015.

[54] A. Petcherdchoo, "Sensitivity of service life extension and CO_2 emission due to repairs by silane treatment applied on concrete structures under time-dependent chloride attack," *Advances in Materials Science and Engineering*, vol. 2018, Article ID 2793481, 10 pages, 2018.